Tree Physiology 00, 1–12
doi:10.1093/treephys/tpaa009

Methods paper

The importance of conduction versus convection in heat pulse sap flow methods

Michael A. Forster[1,2,3]

[1]Implexx Sense, PO BOX 285, Moorabbin, Victoria, 3189, Australia; [2]Edaphic Scientific Pty Ltd, PO BOX 285, Moorabbin, Victoria, 3189, Australia; [3]Corresponding author (michael@edaphic.com.au)

Received October 21, 2019; accepted January 13, 2020; handling Editor Ram Oren

Heat pulse methods are a popular approach for estimating sap flow and transpiration. Yet, many methods are unable to resolve the entire heat velocity measurement range observable in plants. Specifically, the Heat Ratio (HRM) and Tmax heat pulse methods can only resolve slow and fast velocities, respectively. The Dual Method Approach (DMA) combines optimal data from HRM and Tmax to output the entire range of heat velocity. However, the transition between slow and fast methods in the DMA currently does not have a theoretical solution. A re-consideration of the conduction/convection equation demonstrated that the HRM equation is equivalent to the Péclet equation which is the ratio of conduction to convection. This study tested the hypothesis that the transition between slow and fast methods occurs when conduction/convection, or the Péclet number, equals one, and the DMA would be improved via the inclusion of this transition value. Sap flux density was estimated via the HRM, Tmax and DMA methods and compared with gravimetric sap flux density measured via a water pressure system on 113 stems from 15 woody angiosperm species. When the Péclet number $\leq$ 1, the HRM yielded accurate results and the Tmax was out of range. When the Péclet number $>$ 1, the HRM reached a maximum heat velocity at approximately 15 cm hr $^{-1}$ and was no longer accurate, whereas the Tmax yielded accurate results. The DMA was able to output accurate data for the entire measurement range observed in this study. The linear regression analysis with gravimetric sap flux showed an r^2 of 0.541 for HRM, 0.879 for Tmax and 0.940 for DMA. With the inclusion of the Péclet equation, the DMA resolved the entire heat velocity measurement range observed across 15 taxonomically diverse woody species. Consequently, the HRM and Tmax are redundant sap flow methods and have been superseded by the DMA.

Keywords: dual method approach, heat pulse probe, heat ratio method, heat velocity, Péclet number, sap flux density, Tmax, transpiration.

Introduction

Thermal sensors and methods are important tools for understanding plant water relations. Thermal properties are routinely used to estimate sap flux density, transpiration, stem water content and more (Čermák et al. 2004, Smith and Allen 1996). Not only are these parameters fundamental in understanding plant physiology but are increasingly relied upon by industry and policymakers for effective water resource management (Steppe et al. 2015). Therefore, the proper use and deployment of sensors and methods related to thermal properties of plants are essential.

Sap flux density, estimated via the application of heat into or on plant tissue, is primarily measured in the stem's xylem but also other organs from the roots to the peduncle of flowers (Nadezhdina and Čermák 2003, Roddy and Dawson 2012). Popular empirical and theoretical equations to calculate heat velocity in xylem are derived from the theory of conduction and convection of heat in porous materials (Carslaw and Jaeger

1947, Marshall 1958). Following the delivery of heat into the xylem, heat is transferred via conduction, or thermal diffusivity, and/or via the motion of fluid (i.e., sap flow) which is convection. Widely used conduction/convection equations, also referred to as heat pulse equations or methods, include the Tmax and Slow Rates of Flow (SRFM, also known as heat ratio, HRM) methods (Cohen et al. 1981, Marshall 1958, Burgess et al. 2001). These derived formulas are simplified forms of the conduction/convection equation but have been used in many applications including hydraulic plant functioning (Eller et al. 2015, Yu et al. 2018), tree response to elevated carbon dioxide and heatwaves (Zeppel et al. 2011, Pfautsch and Adams 2013), soil–plant–atmosphere continuum models (Deng et al. 2017), phytoremediation (Doronila and Forster 2015), plant–fungi interactions (Forster 2012) and more.

Heat-based sap flow methods are known to unable to measure the entire observable range of heat velocity in plants (Forster 2017, Flo et al. 2019). Heat velocity ranges from approximately −10 cm hr^{-1} (known as reverse flow, or flow from the canopy towards the roots) to > 200 cm hr^{-1} (Forster 2017). Due to constraints on sensor design, electronics, data logging capability and the form of heat transfer equations, it is accepted that various methods optimally describe heat velocity within a restricted range of the overall observable measurement range in plants (Green et al. 2009). Within the heat pulse family of methods, the HRM is optimal at slow and reverse velocities, whereas the Tmax is optimal at moderate to fast velocities (Marshall 1958, Cohen et al. 1988, 1993, Vandegehuchte and Steppe 2013, Forster 2017). The Dual Method Approach (DMA), which incorporates HRM at reverse/slow velocities and Tmax and faster velocities, was demonstrated to successfully resolve the measurement range limitation problem of heat pulse methods (Pearsall et al. 2014, Forster 2019). However, the DMA currently does not have a theoretical method to transition from slow to fast velocity heat transfer equations. In this regard, Pearsall et al. (2014) visually noted the transition, whereas Forster (2019) suggested an empirical and statistical method. A theoretical transition from slow to fast heat transfer equations will improve the DMA.

That the HRM and Tmax optimally describe slow and faster heat velocity suggests these respective methods are describing different aspects of conduction and convection of heat in xylem. Conduction and convection presumably dominate thermal processes at slow to faster velocities, respectively. In thermal physics, the Péclet number is a dimensionless number which describes the ratio of thermal conduction to convection (Bergman et al. 2017). A Péclet number less than or greater than one describes a conductive and convective dominated thermal process, respectively. The Péclet equation is a simple algebraic rearrangement of the HRM equation which is outlined in detail below. Therefore, the Péclet number may provide a theoretical value to transition between slow and fast flows for the DMA.

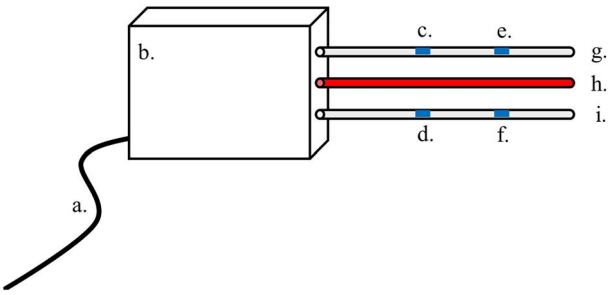

Figure 1. A schematic for a heat pulse probe to measure heat velocity in xylem. (a) Cable to data acquisition system; (b) epoxy body, PCB or analog-digital interface; (c) downstream, outer thermistor (temperature) sensor; (d) upstream outer thermistor; (e) downstream inner thermistor; (f) upstream inner thermistor; (g) downstream temperature probe; (h) heater probe with an internal heating element; (i) upstream temperature probe. The nominal distance between (g) and (h) and (i) and (h) is 0.006 m. The nominal length of the probes is 0.030 m. Not to scale.

In this study, the relative importance of conductive and convective dominated thermal processes was assessed with a large data set including 15 taxonomically diverse woody angiosperm species. A water pressure device was used to artificially impose gradients of sap flux density, from slow to extremely fast, within stems of 15 woody species. The aim of this study was to demonstrate that the HRM and Tmax describe conductive and convective dominated thermal processes, respectively. Consequently, the DMA can be improved via the inclusion of a theoretically derived transition value, the Péclet number, to accurately describe the entire observable measurement range of heat velocity in plants.

Theory and background

The heat pulse probe

The primary focus of this study was on a three-needle design heat pulse probe (Figure 1). The needles must be parallel and, potentially, any equidistance but, practically, are spaced between 0.005 and 0.010 m. The length of the probes can also potentially be any length but in practice is between 0.020 and 0.040 m. The central probe is a line heater, and the downstream (upper) and upstream (lower) probes, in the axial direction, contain one or more paired temperature sensors each. The heat pulse, along the length of the heater needle, ranges between 0.1 and 30 s.

Hereafter, theory, equations and results are made in reference to the sensor design that was deployed in this study. Sensors were the commercially available HPV-06 Heat Pulse Velocity Sensor (Implexx, Melbourne, VIC, Australia). The stainless steel needles had a diameter of 0.0013 m, length of 0.030 m and 0.006 m distance between heater and temperature needles.

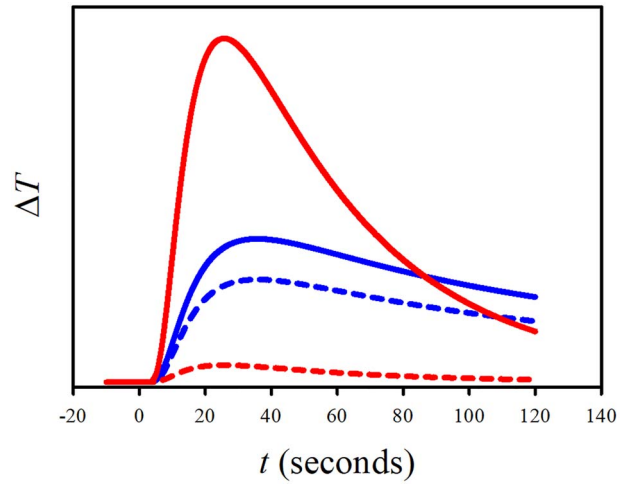

Figure 2. The conduction/convection heat transfer equation showing the change in temperature (ΔT) versus time (t) over a heat pulse measurement cycle. The blue lines show ΔT when heat velocity (V_h) equals 5 cm hr^{-1} and the red lines are V_h equals 45 cm hr^{-1}. The solid and dashed lines are the downstream (i.e., Eq. (1)) and upstream (i.e., Eq. (2)) measurements.

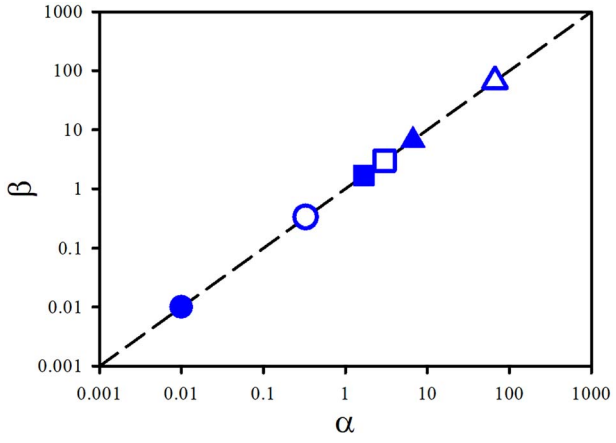

Figure 3. Theoretical thermal equilibrium between the downstream and upstream equidistant temperature needles is demonstrated by the relationship between α and β for a range of heat velocity (V_h). Note that the axes are presented on a log–log scale. The dashed line represents the 1:1 relationship. The figure shows that α always equals β for all V_h which is the definition of thermal equilibrium. Closed circle, V_h = 0.1 cm hr^{-1}; open circle, V_h = 5 cm hr^{-1}; closed square, V_h = 25 cm hr^{-1}; open square, V_h = 45 cm hr^{-1}; closed triangle, V_h = 100 cm hr^{-1}; open triangle, V_h = 1,000 cm hr^{-1}.

Negative temperature coefficient (NTC) thermistors, with an accuracy of ±0.2 °C and a resolution of 0.001 °C, were in each temperature probe at 0.010 m and 0.020 m, respectively. The heater probe had a typical resistance of 38 Ω and dissipated approximately 4 W of power per 3 s heat pulse. Total energy applied per heat pulse was ~400 J m^{-1}.

The conduction/convection heat transfer equation

The two-dimensional conduction/convection heat transfer equations for xylem were outlined by Marshall (1958):

$$\Delta T_d = \frac{q}{4\pi kt} \exp\left[-\frac{(x - V_h t)^2}{4kt}\right] \quad (1)$$

$$\Delta T_u = \frac{q}{4\pi kt} \exp\left[-\frac{(x + V_h t)^2}{4kt}\right] \quad (2)$$

where ΔT is the change in temperature following a heat pulse in the downstream (d- subscript, Eq. (1)) and upstream (u-subscript, Eq. (2)) temperature needles in an axial direction from the heater needle, q is heat input (W m^{-1}), k is thermal diffusivity (m^2 s^{-1}), V_h is heat velocity (m s^{-1}), t is time since heat pulse emission (s) and x is the distance (m) between the heater and temperature needles. Equations (1) and (2) are plotted in Figure 2 for t between −10 and 120 s for V_h values of 5 and 45 cm hr^{-1}.

The V_h and k parameters are the convective and conductive components, respectively, and k is further defined as (Carslaw and Jaeger 1947):

$$k = \frac{K}{\rho c} \quad (3)$$

where K (W m^{-1} K^{-1}) is thermal conductivity and ρ (kg m^{-3}) and c (J kg^{-1} K^{-1}) are the density and heat capacity, respectively, of the sap and wood matrix. The parameters K, ρ and c require further resolution, based on wood and sap properties, stem water content and more, with detailed procedures and calculations provided by Vandegehuchte and Steppe (2012*a*), Looker et al. (2016) and Forster (2019).

Thermal equilibrium and the conduction/convection equation

Thermal equilibrium is defined as the equal change in the ratio of ΔT_d to ΔT_u for all V_h. Resolving Eqs (1) and (2), in combination with the equidistant, three-needle heat pulse probe design (Figure 1), shows that the ratio of ΔT_d to ΔT_u is equal for all V_h (Figure 3). This is thermal equilibrium: the relative change in downstream and upstream temperature needles, post-heat pulse, is in equilibrium for all values of V_h.

In this study, thermal equilibrium is theoretically defined as:

$$\alpha = \beta \quad (4)$$

where

$$\alpha = \ln\left(\frac{\Delta T_d}{\Delta T_u}\right) \quad (5)$$

In practice, pre-heat pulse temperature is an average temperature over some duration prior to the release of the heat pulse (usually 10 s). The post-heat pulse temperature is defined as the average temperature between 60 and 80 s following the heat pulse because this is the convention used for the Heat Ratio Method (HRM, see below for details; Burgess et al. 2001).

The right-hand side of the thermal equilibrium equation is defined as:

$$\beta = \ln\left(\frac{\Delta T_{d,max}}{\Delta T_{u,max}}\right) \quad (6)$$

where $\Delta T_{d,max}$ and $\Delta T_{u,max}$ are the difference between maximum temperature post-heat pulse and the pre-heat pulse temperature in the downstream and upstream temperature needles, respectively.

Thermal equilibrium is demonstrated in Figure 3 which is a plot of α versus β for various values of V_h. At slow heat velocities, where V_h equals 0.1 cm hr^{-1}, α and β equal 0.01. At moderate heat velocities, where V_h equals 25 cm hr^{-1}, α and β equal 1.67. At fast velocities, where V_h equals 1,000 cm hr^{-1}, α and β equal 66.67. That is, for all values of V_h, α and β have a 1:1 ratio, and this is the definition of thermal equilibrium. Furthermore, thermal equilibrium holds for all values q, x and k from Eqs (1) and (2).

Thermal disequilibrium occurs when:

$$\alpha \neq \beta \quad (7)$$

Thermal disequilibrium is significant because it means that the combined utilisation of Eqs (1) and (2) to resolve V_h is invalid. Either Eq. (1) or (2) can be used under conditions of thermal disequilibrium but not together. Under conditions of thermal disequilibrium, Eq. (1) would be used to resolve V_h because it is the heat transfer equation in the downstream direction (i.e., sap flowing from the roots to the canopy).

The Péclet equation and the Péclet number

The Péclet equation, also referred to as the Péclet number, is the ratio of conduction to convection (Wang et al. 2002). When the Péclet number equals one, then conduction and convection are equal. Values less than or greater than a Péclet number of one indicate a conductive or convective dominated process, respectively.

The Péclet equation is (Bergman et al. 2017):

$$Pé = \frac{V_h x}{k} \quad (8)$$

In the context of the Péclet equation, V_h is convection, k is conduction and x is the characteristic length (i.e., the distance between the heater and temperature needles).

The heat ratio (HRM) equation

The HRM is a derived formula from combining Eqs (1) and (2) for characterising heat transfer in the downstream and upstream directions. The HRM equation is:

$$V_h = \frac{\alpha k}{x} \quad (9)$$

A modified version of Eq. (9) was introduced by Kluitenberg et al. (2007) to account for differences in heat pulse duration (t_0) and distance between downstream (x_d) and upstream (x_u) temperature needles from the heater needle:

$$V_h = \frac{2k\alpha}{x_d + x_u} + \frac{x_d - x_u}{t - \left(\frac{t_0}{2}\right)} \quad (10)$$

As the HRM is a combination of Eqs (1) and (2), it is only valid under conditions of thermal equilibrium.

The relationship between thermal equilibrium, Péclet and HRM equations

The Péclet and HRM equations are algebraic re-arrangements of the other. Furthermore, via the inclusion of α and β into the equations, the relationship between thermal equilibrium, the Péclet and HRM equations can be theoretically demonstrated. That is, Eqs (4–6), (8) and (9) are equivalent:

$$Pé = \frac{V_h x}{k} = \alpha = \beta \quad (11)$$

Therefore, the HRM equation describes thermal equilibrium.

The Tmax equation

The Tmax method only requires a two-needle configuration where the temperature needle is positioned downstream to the heater needle (Figure 1). The Tmax formula was outlined by Cohen et al. (1981) as:

$$V_h = \frac{\sqrt{x_d^2 - 4kt_m}}{t_m} \quad (12)$$

where t_m is the time to maximum temperature rise following the heat pulse.

The Tmax formula (Eq. (9)) is highly dependent on an accurate measurement of x_d and heat pulse duration (t_0). Therefore, to account for slight variations in these parameters, Kluitenberg and Ham (2004) and Kluitenberg et al. (2007) proposed the following equation:

$$V_h = \sqrt{\frac{4k}{t_0} ln\left(1 - \frac{t_0}{t_m}\right) + \frac{x_d 2}{t_m\,(t_m - t_0)}} \quad (13)$$

As the Tmax is derived only from Eq. (1), and it requires just a downstream temperature needle, it can theoretically be used under conditions of thermal disequilibrium.

The dual method approach (DMA)

The DMA is an algorithmic technique that utilises the optimal V_h derived from HRM at reverse/slow velocities and Tmax at faster velocities. Forster (2019) suggested two methods to determine the transition between HRM and Tmax based on an a

priori and posteriori determination, ($DMA_{apriori}$ and $DMA_{posteriori}$, respectively).

The $DMA_{apriori}$ technique calculates a $V_{m\_cricital}$ value via the following equation:

$$V_{m\_critical} = \left(\frac{HRM_{\max,k} - Tmax_{\min,k}}{2}\right) + Tmax_{\min,k} \quad (14)$$

where $HRM_{max,k}$ and $Tmax_{min,k}$ are the maximum and minimum measurable V_h for a given k, respectively (Forster 2019).

The transition value in the $DMA_{posteriori}$ technique is determined via a post hoc statistical analysis where measured data is regressed against an independent measure of plant water use such as a weighing lysimeter. A breakpoint statistical method determines an upper threshold V_h from the HRM. The DMA algorithm then takes values below and above the breakpoint threshold from the HRM and Tmax, respectively.

A theoretical transition between HRM and Tmax is preferable as it eliminates bias and can be implemented at the beginning, rather than at the end, of a measurement campaign. In this study, a theoretical threshold/transition value is introduced based on Eq. (11). Values less than or equal to a Péclet number of one correspond to HRM, whereas values greater than one correspond to Tmax. The algorithm for the theoretical DMA method, hereafter called $DMA_{Péclet}$, is:

$$If\,\beta \leq 1\,Then\,V_h = HRM;$$

$$Else\,V_h = Tmax.$$

Wounding and corrected heat velocity (V_c)

Following the correct determination of V_h, it is necessary to correct for sensor installation, as well as sap and wood properties, to calculate sap flux density. The next step after correctly calculating V_h is the calculation of heat velocity corrected for wounding, V_c. A wound correction factor is required due to the insertion of needles into xylem disrupting flow and the formation of tyloses (Swanson and Whitfield 1981, Barrett et al. 1995). V_c (m s^{-1}) is calculated as:

$$V_c = aV_h + bV_h^2 + cV_h^3 \quad (15)$$

where a, b and c are coefficients that are calculated via finite-difference numerical modelling and vary with wound width, probe size and spacing, following Swanson and Whitefield (1981), or values found in the published literature (Swanson and Whitfield 1981, Green and Clothier 1988, Burgess et al. 2001, Green et al. 2003).

Sap flux density (J)

The next step is to convert V_c to sap flux density (J). A common conversion of V_c to J (m^3 m^{-2} s^{-1}; or more commonly expressed as: cm^3 cm^{-2} hr^{-1}) is via (Barrett et al. 1995):

$$J = \frac{V_c \rho_d (c_d + m_c c_w)}{\rho_w c_w} \quad (16)$$

where ρ_d is sapwood dry density (kg kg^{-1}) and c_d and c_w are the specific heat capacity of the dry wood matrix (1200 J kg^{-1} K^{-1}) and sap solution (4182 J kg^{-1} K^{-1}), respectively (Becker and Edwards 1999). ρ_w is the density of sap (assumed to be the density of water, 1000 kg m^{-3}) and m_c is sapwood moisture content (kg kg^{-1}; calculated as: $[w_f—w_d]/w_d$).

Methods

Study species, plant materials and sensor installation

The species that were used in this study are listed in Table 1. Species were chosen based on the availability of material and taxonomic diversity. Species were restricted to woody dicotyledons classified into 15 species, 14 genera and 12 families (Table 1). Plant materials were sourced locally from commercial nurseries where plants were grown on similar substrate and under similar environmental conditions. Within each species, healthy plants between ~0.8 and ~2.0 m height (species dependent) with a basal stem diameter greater than 0.010 m were selected. Depending on the availability of stock, between four and eight stem segments from each species were measured (Table 1).

Prior to cutting of stem samples from the plant, sensors were installed, using a drill guide, into the internodes of stems with diameters between approximately 11 and 13 mm (Table 1). As the effective measurement zone of the thermistors in the temperature probes was 5 mm radius (Forster 2019), the outer paired thermistors were carefully positioned in the stem to at least 5 mm beneath the bark. The sample stem and probes were insulated with foam and aluminium foil to prevent external thermal gradients. Prior to insertion into the stems, the probes were coated with electrical grease (Inox MX6 Grease). Stem samples, of approximately 100 mm length, were then harvested with a sharp pair of secateurs, recut under water and immediately connected to the experimental apparatus to prevent desiccation, embolism or cavitation.

Experimental apparatus

The experimental apparatus was a water pressure system following Forster (2019). The upstream portion of the stem segment was attached to a 13-mm inner diameter Teflon tubing. A watertight seal was created via pipe clamps and polytetrafluoroethylene (PTFE) thread seal tape (Kinetic Supply Pty Ltd, Broadmeadow, Australia) and was tested for leaks prior to measurements. The Teflon tubing was connected to a 10-litre water reservoir to create a constant pressure head. Variable pressure head was created by varying tubing length

Table 1. Summary of species used in this study, their common name, species, variety (if applicable), taxonomic authority, family, the number of stem segments that were measured within species (n), sapwood dry density (ρ_d), thermal diffusivity (k), gravimetric sapwood moisture content (m_c) and wound width including ± standard deviation.

Common name	Species/variety/authority	Family	n	Stem diameter (mm)	Sapwood area (mm^2)	ρ_d ($kg\ m^{-3}$)	k ($cm^2\ s^{-1}$)	m_c ($kg\ kg^{-1}$)	Wound width (mm)
Almond	*Prunus amygdalus* 'Zaione' Batsch	Rosaceae	6	12.3 ± 0.3	69.4 ± 3.1	507 ± 31	0.0025 ± 4 × 10^{-5}	0.897 ± 0.041	2.4 ± 0.1
Apple	*Malus domestica* 'Sweet Cheeks' (Suckow) Borkh.	Rosaceae	8	11.4 ± 0.5	48.1 ± 2.3	547 ± 19	0.0023 ± 3 × 10^{-5}	1.089 ± 0.040	2.0 ± 0.1
Avocado	*Persea americana* 'Hass' Mill.	Lauraceae	8	12.1 ± 0.5	43.2 ± 11.8	534 ± 37	0.0024 ± 1 × 10^{-5}	0.999 ± 0.019	1.7 ± 0.1
Banksia	*Banksia integrifolia* L.f.	Proteaceae	7	11.9 ± 0.6	44.9 ± 5.3	464 ± 33	0.0023 ± 2 × 10^{-5}	1.281 ± 0.068	1.8 ± 0.1
Blueberry	*Vaccinium corymbosum* 'Blue Rose' L.	Ericaceae	8	11.9 ± 0.5	49.3 ± 2.6	496 ± 31	0.0022 ± 8 × 10^{-6}	1.376 ± 0.024	1.9 ± 0.2
Kurrajong	(*Brachychiton populneus* x *discolour* 'Griffith Park' (Schott & Endl.) R.Br.	Sterculiaceae	4	12.7 ± 0.3	51.2 ± 0.6	472 ± 21	0.0025 ± 6 × 10^{-5}	0.872 ± 0.062	2.4 ± 0.1
Mandarin	*Citrus reticulata* 'Emperor' Blanco	Rutaceae	8	12.2 ± 0.5	91.0 ± 4.2	648 ± 54	0.0030 ± 5 × 10^{-5}	0.495 ± 0.026	2.1 ± 0.1
Orange	*Citrus sinensis* 'Valencia' (L.) Osbeck	Rutaceae	8	11.8 ± 0.2	38.2 ± 3.1	587 ± 10	0.0029 ± 6 × 10^{-5}	0.527 ± 0.034	2.2 ± 0.2
Eucalypt	*Eucalyptus mannifera* Mudie	Myrtaceae	8	12.4 ± 0.3	60.6 ± 0.9	425 ± 26	0.0021 ± 2 × 10^{-5}	1.659 ± 0.038	2.1 ± 0.1
Jacaranda	*Jacaranda mimosifolia* D.Don	Bignoniaceae	8	12.1 ± 0.4	42.4 ± 1.9	346 ± 10	0.0024 ± 7 × 10^{-5}	1.128 ± 0.087	2.3 ± 0.1
Bay Tree	*Laurus nobilis* L.	Lauraceae	8	12.6 ± 0.3	24.8 ± 2.3	368 ± 28	0.0023 ± 1 × 10^{-4}	1.307 ± 0.255	1.5 ± 0.1
Mango	*Mangifera indica* 'Bowen' L.	Anacardiaceae	8	12.1 ± 0.7	37.0 ± 5.3	461 ± 33	0.0025 ± 1 × 10^{-4}	0.882 ± 0.113	2.0 ± 0.2
Maple	*Acer palmatum* Thunb.	Aceraceae	8	12.7 ± 0.2	70.9 ± 2.6	544 ± 20	0.0027 ± 4 × 10^{-5}	0.665 ± 0.032	1.6 ± 0.2
Olive	*Olea europaea* 'Kalamata' L.	Oleaceae	8	12.0 ± 0.5	45.4 ± 1.8	530 ± 9	0.0023 ± 1 × 10^{-5}	1.164 ± 0.023	2.2 ± 0.2
Pistachio	*Pistacia chinensis* Bunge	Anacardiaceae	8	11.8 ± 0.7	41.9 ± 1.9	671 ± 49	0.0028 ± 7 × 10^{-5}	0.565 ± 0.046	1.8 ± 0.1

and increasing the height of the reservoir to 150, 400, 900, 1400, 2100, 2600 and 3100 mm.

Stem segments were left to equilibrate for at least 20 min prior to measurements. The sap that exuded downstream of the stem segment was collected at 10-min intervals in a container and immediately weighed on a 3-point balance (WTC 200, Radwag, Radom, Poland).

Stem and wood properties and correction parameters

Immediately following the installation of the excised stem segment with sensor onto the experimental apparatus, an additional small portion of stem, proximate to the excised stem, was sampled for the measurement of thermal diffusivity and sapwood water content. Also, the following stem properties were measured with digital callipers at the sensor installation site: stem diameter, bark depth, sapwood and heartwood radius and sapwood cross-sectional area.

Thermal diffusivity (k) was calculated following the *k_Van* method outlined in detail by Vandegehuchte and Steppe (2012*a*).

Sapwood moisture content (m_c) was determined via the gravimetric technique. The sapwood sample was weighed on the 3-point balance to determine green, wet weight of wood (w_f, kg). The volume (v_f, m^3) was determined via Archimedes' method. The sample was then oven dried 70 °C until a constant weight was reached which was taken as the sapwood dry weight (w_d, kg). Subsequently, sapwood density (ρ_d, kg m^{-3}) was calculated as w_d/v_f. The m_c ($kg\ kg^{-1}$) was calculated as $[w_f—w_d]/w_d$.

Probe misalignment was measured on each installation via the overlength method (Dye et al. 1991). The stainless steel probes protruded through the small stems, and the distance between each probe was measured. Trigonometry was used to calculate the distance between probes within the stem.

Wound diameter was measured at the end of the measurement period. To inspect the wound, the bark, phloem and small portion of the sapwood (approximately 2 mm depth) were carefully removed with a dissecting blade. The calculation of V_c for HRM and Tmax methods, to account for sapwood wounding, was via reference to the published literature (Burgess et al. 2001).

Gravimetric and estimated sap flux density

Gravimetric J was calculated as the gravimetrically weighed sap collected from the experimental apparatus (described above) per sapwood cross-sectional area of each stem segment per hour.

Five heat pulse methods were used in this study to estimate J. Heat velocity was measured via HRM (Eq. (10)), Tmax (Eq. (13)), $DMA_{apriori}$, $DMA_{posteriori}$ and $DMA_{Péclet}$ and were converted to V_c and J, respectively, following the methods described above.

Statistical analysis

The heat pulse methods were evaluated with linear regression statistics that quantify precision and accuracy. Analyses followed Forster (2019) by using linear regression analysis to compare gravimetric J versus estimated J via various heat pulse methods. Linear regression slopes were fitted through the intercept where a slope of one indicates zero error and the r^2 was a measure of precision. A further test of the accuracy of each heat pulse method was conducted via root mean square error (RMSE) where smaller values indicate a more accurate model.

Results

Conductive and convective thermal processes

When data from 15 species were compiled, there was a strong statistical relationship between α and β when the Péclet number was less than one; however, there was a weak relationship when Péclet number was greater than one (Figure 4A). The measured values for α and β, compiled from all 15 species, were significantly correlated when $\beta \leq 1$ with a slope of 1.039 (blue circles in Figure 4A; $r^2 = 0.984$, $n = 464$, $P < 0.001$). When $\beta > 1$, there was a significant correlation between α and β, however, with only 12% of the variation explained and a linear slope of 0.432 (red circles in Figure 4A; $r^2 = 0.120$, $n = 249$, $P < 0.001$).

A theoretical calculation of ΔT_d versus $\Delta T_{d,max}$, calculated from Eq. (1), also showed a 1:1 relationship for all V_h and is represented by the dashed line in Figure 4B. For the measured values from all 15 species, there was a significant linear correlation between ΔT_d and $\Delta T_{d,max}$ with a slope of 0.966 when $\beta \leq 1$ (blue circles in Figure 4B; $r^2 = 0.988$, $n = 465$, $P < 0.001$). When $\beta > 1$, there was a weaker correlation between ΔT_d versus $\Delta T_{d,max}$ where 34.2% of the variation was explained and with a linear slope of 0.785 (red circles in Figure 3b; $r^2 = 0.342$, $n = 254$, $P < 0.001$).

A theoretical calculation of ΔT_u versus $\Delta T_{u,max}$, calculated from Eq. (2), also showed a 1:1 relationship for all V_h and is represented by the dashed line in Figure 4C. For the measured values compiled from the 15 species, there was a significant linear correlation between ΔT_u and $\Delta T_{u,max}$ when $\beta \leq 1$ and $\beta > 1$ (blue circles in Figure 4B; $r^2 = 0.978$, $n = 465$, $P < 0.001$; red circles in Figure 4B; $r^2 = 0.909$, $n = 254$, $P < 0.001$) with a slope of 0.994 and 1.037, respectively.

These results indicate that thermal disequilibrium occurs in the downstream direction when $\beta > 1$, but that thermal equilibrium always occurs in the upstream direction from the heater needle.

Tmax and the Péclet number

The Tmax method calculated valid data when the Péclet number was greater than 0.74. Figure 5A is a breakpoint analysis between t_m and β and indicates there is a breakpoint at $\beta = 0.74$. When $\beta < 0.74$, there is no relationship between t_m and β suggesting that t_m is mostly unrelated to a conductive thermal process. Figure 5B is the relationship between J, estimated via the Tmax method, and β. Figure 5B shows that there were few valid calculations of J, via the Tmax method, when

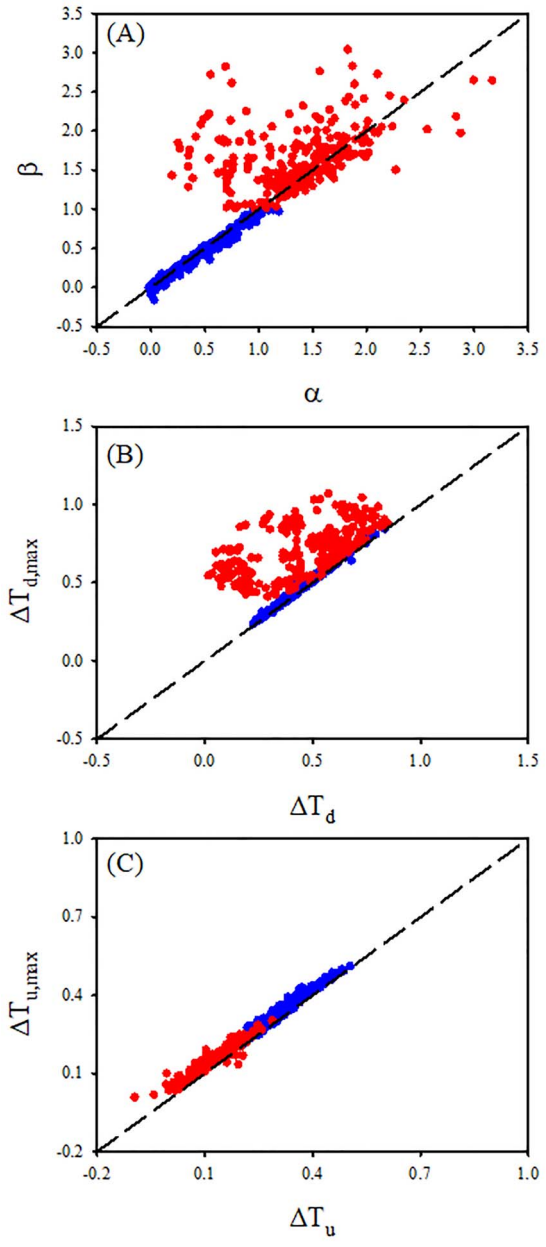

Figure 4. Measured thermal equilibrium and disequilibrium in the xylem of 15 woody species. The blue and red circles are measured data when $\beta \leq 1$ and >1, respectively. The 1:1 relationship is represented by the dashed line. (A) α versus β; (B) $\Delta T_{d,max}$ versus ΔT_d for the downstream temperature needle; (C) $\Delta T_{u,max}$ versus ΔT_u for the upstream temperature needle. Thermal equilibrium occurs when data fall on the 1:1 dashed line which always occurs for the upstream temperature needle. Thermal disequilibrium occurs in α versus β when $\beta > 1$, and this is caused by thermal disequilibrium in the downstream temperature needle.

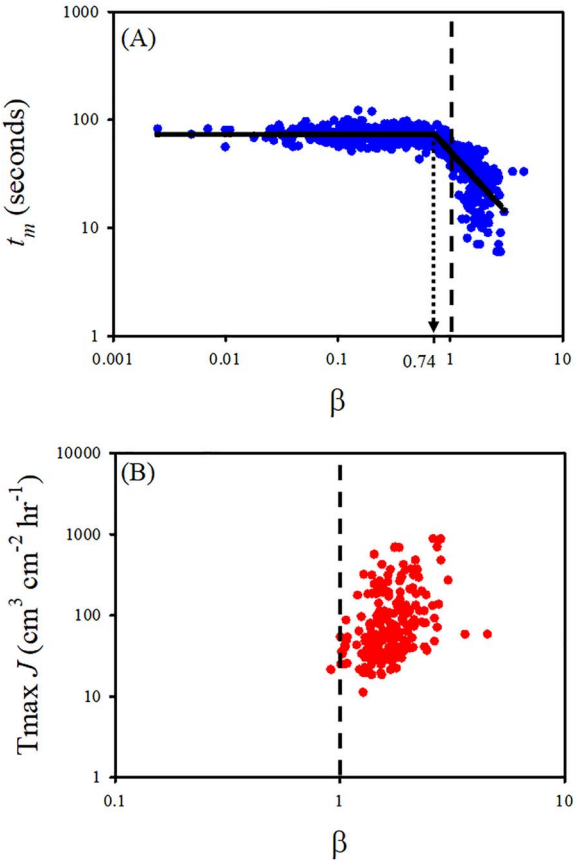

Figure 5. The relationship between (A) t_m and β and (B) sap flux density (J, estimated via the Tmax method) and β. A breakpoint statistical analysis (solid black line) indicated that there was a significant linear relationship between t_m and β when $\beta > 0.74$ (dotted line in A). The dashed line indicates where $\beta = 1$ which is when conduction equals convection. In this study, when $\beta < 1$, the Tmax method recorded an out of range or invalid value that could not calculate V_h and J. The Tmax method only produced a valid value when $\beta > 1$, suggesting this method describes a convective dominated process. Note the log scaling on all axes.

$\beta < 1$ which also indicates that the Tmax method is unrelated to a conductive thermal process.

Heat pulse methods and the estimation of sap flux density

The HRM, Tmax and DMA methods underestimated gravimetrically measured J (Figure 6 and Table 2). The HRM showed the largest error and poorest precision and underestimated gravimetric J by 63.3% (Table 2). The maximum measurement range of the HRM was 73.3 (cm^3 cm^{-2} hr^{-1}) versus an observed maximum gravimetric J of 2007 (cm^3 cm^{-2} hr^{-1}). These results indicate that the HRM was inaccurate at estimating faster V_h and J.

The Tmax method was the least accurate method in terms of RMSE (Table 2). Additionally, the Tmax method was out of range for 5 of the 15 species. The Tmax had a maximum J measurement range of 873.8 (cm^3 cm^{-2} hr^{-1}) but a minimum range of 11.1 (cm^3 cm^{-2} hr^{-1}). These results indicate that the Tmax method was unable to resolve slower V_h and J.

The DMA$_{apriori}$ method also underestimated J with an error of 60.7%, although it was as a better method, in terms of RMSE, than the HRM and Tmax methods (Table 2).

The DMA$_{posteriori}$ and DMA$_{Péclet}$ methods had the same maximum and minimum measurement range of 873.8 and 0 (cm^3 cm^{-2} hr^{-1}), respectively. The results from the DMA$_{posteriori}$ and DMA$_{Péclet}$ methods were similar for all statistical parameters listed in Table 2 indicating these two methods described the same underlying process.

Figure 6 shows the relationship between gravimetric J and estimated J via heat pulse methods. For better visual representation of the results, only data within the range of 200 cm^3 cm^{-2} hr^{-1} is displayed. Figure 6A shows the HRM data reached a plateau at approximately 30 cm^3 cm^{-2} hr^{-1}, whereas Figure 6B shows the Tmax did not produce any results less than approximately 11 cm^3 cm^{-2} hr^{-1}. Figure 6C indicated that the DMA$_{apriori}$ method resolved a wider range of J but had large scatter. Figure 6D indicated that the DMA$_{Péclet}$ method resolved the full range of J observed in these data. The DMA$_{posteriori}$ data were not displayed as they were statistically similar to the DMA$_{Péclet}$ data.

Discussion

Sap flow methods based on heat transfer equations are known to unable measure the entire observable range of heat velocity in plants. By testing various heat pulse methods on a large data set of 15 woody species, this study demonstrated that the theoretically derived Dual Method Approach (DMA$_{Péclet}$) can resolve the entire measurement range of heat velocity in plants. This study also demonstrated the importance of differentiating between conductive and convective dominated processes when using thermal methods to estimate sap flux density. By explicitly recognising conductive and convective processes, this study was also the first to theoretically explain the limitations of the Heat Ratio Method (HRM) at moderate to fast velocities.

Conductive and convective dominated processes

The conduction/convection heat transfer equations have been used to estimate sap flow in plants since at least the 1930s (Huber 1932, Marshall 1958). The implicit understanding has been that the equation differentiates between a conduction component (i.e., thermal diffusivity, k) and a convective component (i.e., heat velocity, V_h). However, the results from this study suggested that it is not a dichotomy between conduction and convection, but a continuum from a conductive to a convective dominated process. However, the Péclet number does not eliminate convection when conduction is dominant or conduction when convection is dominant. Rather, there is a spectrum, or continuum, where one process supersedes the other process when the Péclet number is equal to one.

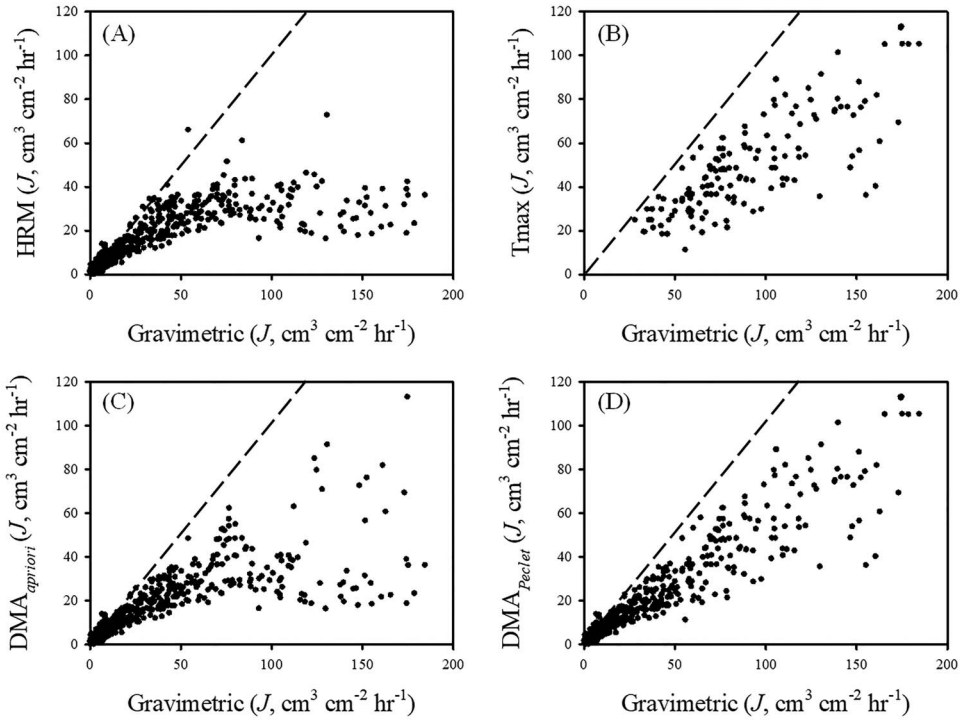

Figure 6. Sap flux density (*J*) compiled from the 15 species measured via the gravimetric technique versus *J* estimated via four heat velocity methods: (A) HRM; (B) Tmax; (C) $DMA_{apriori}$; (D) $DMA_{Péclet}$. The dashed line represents the 1:1 relationship between estimated and gravimetric *J*. Note that the $DMA_{posteriori}$ and $DMA_{Péclet}$ data were identical so only the $DMA_{Péclet}$ data were presented. Results from the linear regression analysis were presented in Table 2. The figure shows the (A) HRM method reaches a maximum limit and cannot measure faster *J*, whereas (B) Tmax has missing data at slow *J*. The (D) $DMA_{Péclet}$ method can resolve the entire range of *J* observed in these data.

Table 2. The accuracy of a heat pulse method in estimating gravimetrically measured sap flux density (*J*). Values are the average and ± standard deviation from each of the 15 woody species (*n*). Slope is derived from the linear regression of a heat pulse method against gravimetric J with the intercept forced through zero. Error is the percent deviation of the slope from one. RMSE is the root mean square error of the method with lower values indicating a more accurate result. The maximum and minimum ranges are the measured *J* for each method.

Method	Slope	Error (%)	R^2	RMSE	Max. range ($cm^3\ cm^{-2}\ hr^{-1}$)	Min. range ($cm^3\ cm^{-2}\ hr^{-1}$)	*n*
Gravimetric					2007.0	0.2	15
HRM	0.367, ±0.055	63.3, ±5.5	0.541, ±0.099	96.0, ±44.1	73.3	0.0	15
Tmax	0.510, ±0.038	49.0, ±3.8	0.879, ±0.031	108.2, ±39.7	873.8	11.1	10
$DMA_{apriori}$	0.393, ±0.053	60.7, ±5.3	0.622, ±0.088	92.6, ±43.3	184.3	0.0	15
$DMA_{posteriori}$	0.525, ±0.031	47.5, ±3.1	0.939, ±0.012	62.3, ±26.9	873.8	0.0	15
$DMA_{Péclet}$	0.523, ±0.031	47.7, ±3.1	0.940, ±0.012	61.9, ±27.0	873.8	0.0	15

The measurement range limitation of heat pulse methods

Previous attempts to resolve the measurement range limitation of heat pulse methods used theoretical, empirical and statistical methods. These methods have varying degrees of success and difficulty of implementation. The theoretical method introduced in this study to resolve heat velocity measurement range limitations, the $DMA_{Péclet}$ method, is relatively simple to implement which contrasts with another theoretical method, the Sapflow+ method (Vandegehuchte and Steppe 2012*b*). To resolve heat velocity measurement range limitations, Sapflow+ is mathematically and computationally complex and requires potentially elaborate hardware and third-party software, which limits its practical use (Forster 2017). Empirical methods, which also aim to resolve heat velocity measurement range limitations, such as the various empirical gradients methods (Testi and Villalobos 2009, Green and Romero 2012, Romero et al. 2012), require complex and laborious post hoc handling of data which also limits their practical use. Statistical methods, such as $DMA_{posteriori}$ (Forster 2019), can only be implemented as a post hoc analysis with an independent measure of sap flow (Forster 2019). In this study, the results from the $DMA_{Péclet}$ method were similar to the $DMA_{posteriori}$ method, meaning that a theoretical and statistical method can produce similar outcomes.

Moreover, the results of this study are the first to theoretically explain the measurement range limitations of the HRM in the context of sap flow in plants but have previously been explored

Table 3. Maximum V_h values for the HRM for various k. The maximum V_h is calculated via Eq. (9) when the Péclet number equals one (i.e., α equals one) and x equals 0.6 cm. Values higher than the maximum Vh, returned via the HRM, are unreliable due to thermal disequilibrium and cannot be used for subsequent estimates of sap flux density and sap flow.

k (cm^2 s^{-1})	V_h (cm hr^{-1})
0.0015	9
0.0020	12
0.0025	15
0.0030	18
0.0035	21
0.0040	24

in the context of water flux in soils (Wang et al. 2002). It is known that the HRM cannot resolve moderate to high heat velocities (Bleby et al. 2008). Yet, a theoretical understanding of the problem was unknown. This study mathematically and experimentally demonstrated that the HRM is valid when there is thermal equilibrium between the downstream and upstream measurement points, and this occurs when the Péclet number is less than one. Under conditions of thermal disequilibrium (i.e., when Péclet number > 1), the α parameter in the HRM equation is extremely variable. This is demonstrated by the large scatter in values in Figure 4A when $\alpha > 1$. This extreme uncertainty over whether α has been correctly determined means the HRM is unreliable at higher heat velocities.

The violation of thermal equilibrium occurred in the downstream temperature probe, whereas the upstream temperature probe conformed to thermal equilibrium (Figure 4B and C). This contrasted with previous speculation that it was a dampening in the upstream temperature signal that is the problem with HRM at high velocities (Vandegehuchte and Steppe 2013). Furthermore, Marshall (1958) and Burgess et al. (2001) noted, without a theoretical explanation, that the maximum $\Delta T_d/\Delta T_u$ value for HRM was 20, whereas Forster (2019) speculated that the $\Delta T_d/\Delta T_u$ value did not exceed 5. The maximum $\Delta T_d/\Delta T_u$ is actually 2.72 which is when the Péclet number equals one (i.e., $\ln(2.72)$ equals 1). The Péclet number of one translates to a maximum V_h of approximately 9–24 cm hr^{-1} depending on k and with a probe spacing (x) of 0.6 cm (Table 3). Therefore, any study that presents, or has presented, V_h or J data derived from HRM where the $\ln(\Delta T_d/\Delta T_u)$ is greater than one should be treated with extreme caution.

The Tmax method, on the other hand, produced valid data when convection was a dominant thermal process. In this study, V_h calculated via Tmax was valid when the Péclet number was approximately greater than one or when V_h was faster than approximately 10 cm hr^{-1}. This result for minimum velocity was also found in other studies (Green et al. 2009, Vandegehuchte and Steppe 2013, Morton et al. 2016, Forster 2019) and was explained by limitations in electronics, small temperature drifts and a non-unique relationship between t_m and V_h at slow flows (Becker 1998, Green et al. 2003, Vandegehuchte and Steppe 2013). In contrast, the timing limitation of Tmax at slow velocity is an advantage at faster velocities where t_m is easily resolved with contemporary electronics. Therefore, the Tmax method can resolve moderate to faster velocities.

This study demonstrated that the $DMA_{Péclet}$ can theoretically measure a wide range of V_h observed in plants. The HRM and Tmax methods, in contrast, can only measure a restricted portion of the V_h range. It was mathematically, technically and statistically demonstrated that using either the HRM or Tmax in isolation will result in the likely misinterpretation of sap flow results. If the HRM or Tmax is used to measure heat velocity, without reference to another wider range of heat pulse method, then there is an implicit risk of error. Instead, the $DMA_{Péclet}$ is a theoretically derived method, which incorporates the respective strengths of the HRM and Tmax methods and removes the chance of errors in heat velocity measurements.

Observed heat velocity and sap flux density values

Measured heat velocity (V_h) in this study ranged between 0 and ~500 cm hr^{-1} for *Eucalyptus mannifera*, but the other 14 species in this study had maximum $V_h < 200$ cm hr^{-1}. These values compare with previous studies using heat pulse probes including 150 cm hr^{-1} in plane tree (Morton et al. 2016), ~200 cm hr^{-1} in grapevines (Pearsall et al. 2014) and 266.4 cm hr^{-1} in soybean (Cohen et al. 1993).

The higher values observed in this study resulted from the application of water flow on cut stems. The sampled stems were effectively open pipes with little hydraulic resistance (Sperry et al. 2003). For the purposes of this study, it was inconsequential that the experimental apparatus artificially imposed higher rates of sap flux than may be reasonably expected under natural conditions. The main aim of this study was to test heat transfer equations over a wide measurement range. Therefore, the water pressure experimental design was chosen to recreate sap flux likely encountered by plants as well as artificially high conditions which was successfully achieved.

Underestimation of sap flux density

In this study, the conversion of V_h to J, via the $DMA_{Péclet}$, as well as HRM and Tmax methods, underestimated gravimetric J. The underestimation of J has been widely noted for many thermal sap flow methods (Forster 2017, Flo et al. 2019) and was confirmed for all 15 woody species measured in this study.

The underestimation problem is not a result of the heat transfer equations that form the basis of sap flow methods. The heat transfer equations show the correct relationship between sap and heat velocity (Wang et al. 2002, Jones et al. 1988). The underestimation problem is caused via the conversion of V_h to J. For example, the wound correction factor was proposed to correct for the underestimation problem and has been incorpo-

rated in many studies (e.g., Green and Clothier 1988, Burgess et al. 2001, Green et al. 2003). Although wound correction does improve the accuracy of J estimates (Green et al. 2009), and its incorporation has improved heat pulse methods over other methods such as thermal dissipation (Flo et al. 2019), numerous studies have nevertheless demonstrated that wound correction does not lead to accurate J estimates (Forster 2017). For example, despite including a wound correction, Wang et al. (2015) measured a ~42% underestimation via HRM on a *Salix matsudana*, and González-Altozano et al. (1998) observed a 31% underestimation via Tmax on a citrus species. This study found a similar result as wound correction was carefully measured, yet there was an underestimation of J in all 113 sampled stems across 15 species. It was possible that the wound size was not precisely measured in these, or other, studies. However, the inclusion of a wider range of wound correction values on the data in this study did not resolve the underestimation problem (data not shown). Similarly, Wang et al. (2015) artificially adjusted their wound correction to improve their data but cautioned against this approach. If wound correction is intended to resolve the underestimation problem, then the results of this and numerous other studies suggest that the wound correction procedure is incomplete and requires further development. Another potential source of error is variation in sapwood moisture content (m_c) and the subsequent inaccuracies this causes on the calculations of thermal diffusivity (k) and J (Green et al. 2009, Steppe et al. 2010). Yet, the experimental design deployed in this study presumably caused no or, at least, minimal variation in m_c to explain the underestimation of measured versus observed J. Therefore, it is probable that another factor caused the systematic underestimation of measured J observed in this study.

Conclusion

A re-evaluation of the conduction/convection equation demonstrated that popular heat pulse sap flow methods describe either a conductive (HRM) or convective (Tmax) dominated process. Consequently, the HRM and Tmax methods are limited in their ability to resolve the entire range of observable heat velocity in plants. The $DMA_{Péclet}$ method improved previous empirical and statistical DMA methods via the inclusion of a theoretically derived transition value when the ratio of conduction to convection, i.e., the Péclet number, is equal to one. The $DMA_{Péclet}$ was able to resolve slow and fast heat velocity, and it is recommended this method is used as a replacement for the HRM and Tmax methods.

Conflict of Interest

The author is the owner of a company which manufactures and distributes the sap flow sensors that were used in this study.

References

Barrett DJ, Hatton TJ, Ash JE, Ball MC (1995) Evaluation of the heat pulse velocity technique for measurement of sap flow in rainforest and eucalypt forest species of South-Eastern Australia. Plant Cell Environ 18:463–469.

Becker P (1998) Limitations of a compensation heat pulse velocity system at low sap flow: implications for measurements at night and in shaded trees. Tree Physiol 18:177–184.

Becker P, Edwards WRN (1999) Corrected heat capacity of wood for sap flow calculations. Tree Physiol 19:767–768.

Bergman TL, Lavine AS, Incropera FP, DeWitt DP (2017) Fundamentals of heat and mass transfer, 8th edn. NJ John Wiley & Sons, Inc., Hoboken, USA.

Bleby TM, McElrone AJ, Burgess SSO (2008) Limitations of the HRM: Great at low flow rates, but not yet up to speed? In Proceedings of the 7th International Workshop on Sap Flow: Book of Abstracts, Seville, Spain, 22–24 October 2008.

Burgess SSO, Adams MA, Turner NC, Beverly CR, Ong CK, Khan AAH, Bleby TM (2001) An improved heat pulse method to measure low and reverse rates of sap flow in woody plants. Tree Physiol 21: 589–598.

Carslaw HS, Jaeger JC (1947) Conduction of heat in solids. Oxford University Press, London: UK.

Čermák J, Kučera J, Nadezhhdina N (2004) Sap flow measurements with some thermodynamic methods, flow integration within trees and scaling up from sample trees to entire forest stands. Trees 18:529–546.

Cohen Y, Fuchs M, Falkenflug V, Moreshet S (1988) Calibrated heat pulse method for determining water uptake in cotton. Agron J 80:398–402.

Cohen Y, Fuchs M, Green GC (1981) Improvement of the heat pulse method for determining sap flow in trees. Plant Cell Environ 4:391–397.

Cohen Y, Takeuchi S, Nozaka J, Yano T (1993) Accuracy of sap flow measurements using heat balance and heat pulse methods. Agron J 85:1080–1086.

Deng Z, Guan H, Hutson J, Forster MA, Wang T, Simmons CT (2017) A vegetation focused soil-plant-atmospheric continuum model to study hydrodynamic soil-plant water relations. Water Resour Res 53:4965–4983.

Doronila AI, Forster MA (2015) Performance measurement via sap flow monitoring of three eucalyptus species for mine site and dryland salinity phytoremediation. Int J Phytoremediation 17: 101–108.

Dye PJ, Olbrich BW, Poulter AG (1991) The influence of growth rings in *Pinus patula* on heat pulse velocity and sap flow measurements. J Exp Bot 42:867–870.

Eller CB, Burgess SSO, Oliveira RS (2015) Environmental controls in the water use patterns of a tropical cloud forest tree species, *Drimys brasiliensis* (Winteraceae). Tree Physiol 35:387–399.

Flo V, Martinez-Vilalta J, Steppe K, Schuldt B, Poyatos R (2019) A synthesis of bias and uncertainty in sap flow methods. Agric For Meteorol 271:362–374.

Forster MA (2012) Quantifying water use in a plant-fungal interaction. Fungal Ecol 5:702–709.

Forster MA (2017) How reliable are heat pulse velocity methods for estimating tree transpiration? Forests 8:350.

Forster MA (2019) The dual method approach (DMA) resolves measurement range limitations of heat pulse velocity sap flow sensors. Forests 10:46.

Gonzalez-Altozano P, Ruiz-Sin B, Castel JR (1998) Sap flow determination in citrus trees by heat pulse techniques. In: Proceedings of the Fourth International Workshop on Measuring Sap Flow in Intact Plants. Zidlochovice, Czech Republic, 3–4 November.

Green S, Clothier B, Perie E (2009) A re-analysis of heat pulse theory across a wide range of sap flows. Acta Hort 846:95–103.
Green SR, Clothier B, Jardine B (2003) Theory and practical application of heat pulse to measure sap flow. Agron J 95:1371–1379.
Green SR, Clothier BE (1988) Water use of kiwifruit vines and apple trees by the heat-pulse technique. J Exp Bot 39:115–123.
Green SR, Romero R (2012) Can we improve heat-pulse to measure low and reverse flows? Acta Hort 951:19–29.
Huber B (1932) Beobachtung und messung pflanzlicher Saftströme. Berichte der Deutschen Botanischen Gesellschaft 50:89–109.
Jones HG, Hamer PJC, Higgs KH (1988) Evaluation of various heat-pulse methods for estimation of sap flow in orchard trees: comparison with micrometeorological estimates of evaporation. Trees 2:250–260.
Kluitenberg GJ, Ham JM (2004) Improved theory for calculating sap flow with the heat pulse method. Agric For Meteorol 126:169–173.
Kluitenberg GJ, Ochsner TE, Horton R (2007) Improved analysis of heat pulse signals for soil water flux determination. Soil Sci Soc Am J 71:53–55.
Looker N, Martin J, Jencso K, Hu J (2016) Contribution of sapwood traits to uncertainty in conifer sap flow as estimated with the heat-ratio method. Agric For Meteorol 223:60–71.
Marshall DC (1958) Measurement of sap flow in conifers by heat transport. Plant Physiol 33:385–396.
Morton D, Ghayvat H, Mukhopadhyay SC, Green S (2016) Sensors and instrumentation to measure sap flow in small stem plants. 2016 IEEE International Instrumentation and Measurement Technology Conference Proceedings. Taipei, Taiwan.
Nadezhdina N, Čermák J (2003) Instrumental methods for studies of structure and function of root systems of large trees. J Exp Bot 54:1511–1521.
Pearsall KR, Williams LE, Castorani S, Bleby TM, McElrone AJ (2014) Evaluating the potential of a novel dual heat-pulse sensor to measure volumetric water use in grapevines under a range of flow conditions. Func Plant Biol 41:874–883.
Pfautsch S, Adams MA (2013) Water flux of *Eucalyptus regnans*: defying summer drought and a record heatwave in 2009. Oecologia 172:317–326.
Roddy AB, Dawson TE (2012) Determining the water dynamics of flowering using miniature sap flow sensors. Acta Hort 951: 47–54.
Romero R, Muriel JL, Garcia I, Green SR, Clothier BE (2012) Improving heat-pulse methods to extend the measurement range including reverse flows. Acta Hort 951:31–38.
Smith DM, Allen SJ (1996) Measurement of sap flow in plant stems. J Exp Bot 47:1833–1844.
Sperry JS, Stiller V, Hacke UG (2003) Xylem hydraulics and the soil-plant-atmosphere continuum: opportunities and unresolved issues. Agron J 95:1362–1370.
Steppe K, De Pauw DJW, Doody TM, Teskey RO (2010) A comparison of sap flux density using thermal dissipation, heat pulse velocity and heat field deformation methods. Agric For Meteorol 150: 1046–1056.
Steppe K, Vandegehuchte MW, Tognetti R, Mencuccini M (2015) Sap flow as a key trait in the understanding of plant hydraulic functioning. Tree Physiol 35:341–345.
Swanson RH, Whitfield DWA (1981) A numerical analysis of heat pulse velocity and theory. J Exp Bot 32:221–239.
Testi L, Villalobos F (2009) New approach for measuring low sap velocities in trees. Agric For Meteorol 149:730–734.
Vandegehuchte MW, Steppe K (2012a) Improving sap-flux density measurements by correctly determining thermal diffusivity, differentiating between bound and unbound water. Tree Physiol 32:930–942.
Vandegehuchte MW, Steppe K (2012b) Sapflow+: a four-needle heat pulse sap flow sensor enabling nonempirical sap flux density and water content measurements. New Phytol 196:306–317.
Vandegehuchte MW, Steppe K (2013) Sap-flux density measurement methods: working principles and applicability. Func Plant Biol 40:213–223.
Wang Q, Ochsner TE, Horton R (2002) Mathematical analysis of heat pulse signals for soil water flux determination. Water Resour Res 38:271–277.
Wang S, Fan J, Wang Q (2015) Determining evapotranspiration of a Chinese willow stand with three-needle heat-pulse probes. Soil Sci Soc Am J 79:1545–1555.
Yu T, Feng Q, Si J, Mitchell PJ, Forster MA, Zhang X, Zhao C (2018) Depressed hydraulic redistribution of roots more by stem refilling than by nocturnal transpiration for *Populus euphratica* Oliv in situ measurement. Ecol Evol 8:2607–2616.
Zeppel MJB, Lewis JD, Medlyn B et al. (2011) Interactive effects of elevated CO_2 and drought on nocturnal water fluxes in *Eucalyptus saligna*. Tree Physiol 31:932–944.